CrossMark

ORIGINAL PAPER

# Enhanced electrocatalytic determination of fenitrothion at graphene and silver–zirconia nanosensor

N. Y. Sreedhar · M. Sunil Kumar · K. Krishnaveni

Abstract A nanocomposite sensor based on Ag-ZrO$_2$ nanoparticles and graphene was fabricated and employed for electrocatalytic detection of fenitrothion. Improved electrocatalytic activity of the sensor was demonstrated by cyclic voltammetry and impedance techniques. In fenitrothion, electrochemical reduction of the nitro group to hydroxylamine was found to be irreversible, adsorption-controlled, and pH dependent. Improved voltammetric peak signals for fenitrothion were obtained due to the synergistic effect of silver and zirconia nanoparticles over graphene support. Square wave adsorptive stripping voltammetric method was developed for highly sensitive determination of fenitrothion. Working conditions such as pH, accumulation potential, accumulation time, square wave frequency, square wave amplitude, and scan rate were optimized with respect to maximum and well-defined peak signals. Wide linear range was observed between the peak signals and concentration of fenitrothion over the range 0.1–100 nM with a detection limit of 0.56 nM. The proposed stripping voltammetric protocol is readily applied for the determination of fenitrothion in well water and soil samples with good recoveries.

Graphical abstract
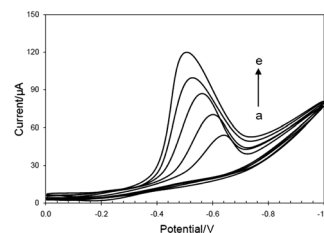
Keywords Graphene · Ag and ZrO$_2$ nanoparticles · Square wave voltammetry · Fenitrothion · Well water and soil samples

Introduction

Organophosphate pesticides are one of the most widely used synthetic organic pesticides in agriculture and other commercial activities due to their effectiveness over a wide range of insects and pests. Fenitrothion, an active member of OP family with chemical structure as shown in Fig. 1, is mainly used against flies, mosquitoes, and locusts besides a variety of chewing and sucking insects. It is readily degradable and hence less persistent in environment than organochlorine pesticides. However, residues of fenitrothion are reported to be highly toxic to non-target species such as birds, mammals, and aquatic life [1–3]. Its carcinogenic and mutagenic effects are derived from its partial intercalative interaction with DNA [4]. Hence regular monitoring of fenitrothion is a requisite for the control of its environmental pollution. Analytical techniques usually employed are based on gas chromatography (GC), high-performance liquid chromatography (HPLC), enzyme

N. Y. Sreedhar (✉) · M. Sunil Kumar · K. Krishnaveni
Department of Chemistry, Electroanalytical Lab,
Sri Venkateswara University, Tirupati 517502,
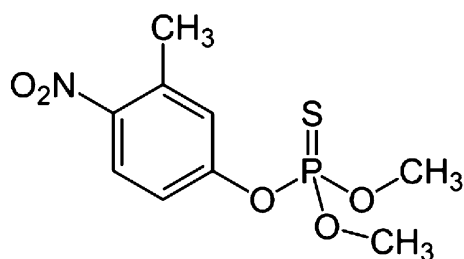Andhra Pradesh, India
e-mail: nyschem01@gmail.com

Springer

Fig. 1 Chemical structure of fenitrothion

linked immunosorbent assay (ELISA), and spectrofluorometry [5–14]. Most of the above methods are costly, effort- and time-demanding procedures with multiple sample preparation and measurement steps.

Based on their simplicity, low-cost, and sensitivity, a few polarographic methods were developed for the determination of fenitrothion [15, 16]. Fenitrothion and its metabolites in river water samples were simultaneously determined by adsorptive stripping square wave voltammetry with second-order multivariate calibration [17]. A wide variety of modified electrodes, namely nano-TiO_2 polymer film modified glassy carbon electrode (GCE), carbon ceramic electrode, molecular imprinted polymer based screen printed electrode, nano TiO_2/Nafion composite, polyaniline modified GCE, electrochemically pretreated GCE, functionalized multiwalled carbon nanotubes (MWNTs) modified GCE, and poly(4-amino-3-hydroxynaphthalenesulfonic acid) modified GCE were developed for the determination of fenitrothion [18–25]. Most of the above electrodes offer narrow working ranges with high detection limits. Hence to improve analytical figures of merit, there exists a need for highly sensitive sensors for early detection and accurate determination of fenitrothion in environmental matrices.

Graphene is a latest member of the ever-increasing class of carbon nanomaterials which is mainly composed of hexagonal carbon framework with two-dimensional, one-atom thick, sheet-like structure. The material has wide range of applications owing to its unique properties such as high surface area, good electrical conductivity, fast electron transfer, and excellent catalytic activity. A plethora of sensors based on graphene and its composites using metal nanoparticles, redox polymers were developed for the determination of molecules of biological significance [26, 27]. Metal nanoparticles are often used in sensor design for different analytes owing to their special optical, mechanical, chemical, and electrical properties [28–32]. High sensitivities are obtained for silver and zirconia nanoparticles based sensors owing to their high catalytic activities [33, 34]. Among the wide variety of nanocomposites being developed, graphene and metal nanoparticles occupy a prominent position in electroanalysis since they bring out

pronounced synergistic effect of individual components in the detection of significant analytes. A variety of graphene–metal composite sensors and biosensors were used for accurate determination of OP pesticides with wide linear range and low detection limits [35–38].

The present work is, therefore, devoted to the fabrication of a non-enzymatic, sensitive sensor for fenitrothion based on Ag and ZrO_2 nanoparticles over graphene framework. The nanocomposite is electrochemically characterized by cyclic voltammetry and impedance studies. It is then employed for the development of square wave adsorptive stripping voltammetric determination of fenitrothion to obtain high sensitivity, good linearity, and low detection limits. The practical utility of the analytical method is demonstrated by its successful application to well water and soil samples.

Results and discussion

Electrochemical characterisation of Ag-ZrO$_2$-GR/GCE

By cyclic voltammetry (CV), the electrochemistry of the modified electrode was studied with respect to the redox probe, $[Fe (CN)_6]^{3-/4-}$. A working solution of the potassium ferricyanide (1 mM) was prepared in KCl (0.1 M) solution that acts as supporting electrolyte. A triangular potential scan from 0.0 to +0.5 V was applied to Ag-ZrO_2-GR/GCE at a scan rate of 50 mVs^{-1}. The peak currents and peak separations for each electrode were compared with present nanocomposite electrode. As shown in Fig. 2, peak to peak separation (ΔE_p) values for bare GCE (a), GR/GCE (b), Ag-GR/GCE (c), ZrO_2-GR/GCE (d), and Ag-ZrO_2-GR/GCE (e) were 110, 92, 84, 70, and 61 mV, respectively. Again peak currents at the nanocomposite increased by almost 5 times to that of bare GCE. Enhanced and well-defined peaks were obtained with low ΔE_p value for Ag-ZrO_2-GR/GCE implying high electrical conductivity and fast electron transfer kinetics. The active surface area of the nanocomposite can be obtained using the following Randles- Sevcik equation

$$i_p = 2.69 \times 10^5 n^{3/2} A D^{1/2} C v^{1/2}, \tag{1}$$

where A is the area of the electrode in cm^2, D is the diffusion coefficient for $[Fe (CN)_6]^{3-} = 7.6 \times 10^{-6}$ cm^2/s (at $T = 298$ K), n is the no. of electrons $= 1$, C is the concentration of $[Fe (CN)_6]^{3-} = 1$ mM, and v is the scan rate in mV/s. The surface area of bare GCE, GR/GCE, Ag-GR/GCE, ZrO_2-GR/GCE, and Ag-ZrO_2-GR/GCE were found to be 0.061, 0.124, 0.215, 0.252, and 0.395 cm^2, respectively.

Electron transfer resistance of the present nanocomposite can be studied using electrochemical impedance
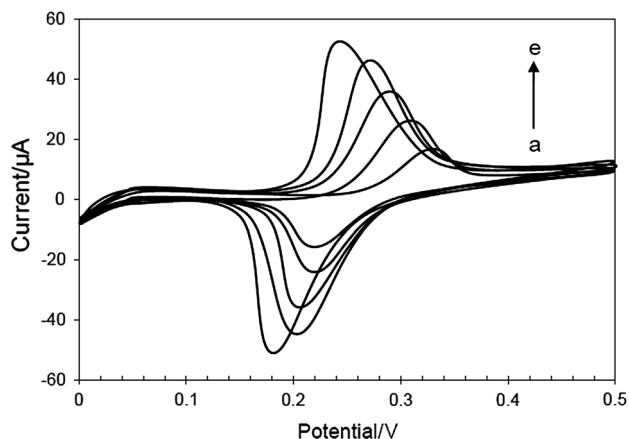
Fig. 2 Cyclic voltammograms of **a** bare GCE, **b** GR/GCE, **c** Ag-GR/GCE, **d** ZrO$_2$-GR/GCE, and **e** Ag-ZrO$_2$-GR/GCE (**e**) in the presence of ferricyanide (1 mM) with 0.1 M KCl (pH 3.0) at a scan rate of 50 mVs^{-1}

technique which demonstrates the electron conduction pathways for nanocomposite interface in the presence of redox probe molecule. Electrochemical impedance spectral studies (EIS) were carried out for Ag-ZrO$_2$-GR/GCE (**e**) along with different electrodes such as ZrO$_2$-GR/GCE (**d**), Ag-GR/GCE (**c**), GR-GCE (**b**), and bare GCE (**a**) in the presence of potassium ferricyanide (5 mM) in 0.1 M KCl solution at frequencies of 0.1 Hz to 10^5 Hz. Nyquist plots were constructed with impedance real (Z_{re}) on x-axis and impedance imaginary (Z_{im}) on y-axis. As given in Fig. 3, the plots consist of semicircular part, the diameter of which gives the electron transfer resistance (R_{et}) of the electrode interface. Reduced semi-circular diameter (110 Ω) was observed for Ag-ZrO$_2$-GR/GCE compared to ZrO$_2$-GR/GCE (160 Ω), Ag-GR/GCE (240 Ω), GR/GCE (320 Ω), and bare GCE (430 Ω). This clearly indicates that electron transfer is faster at the nanocomposite sensor due to increased surface-volume ratio and electrical conductivity of modified nanocomposite layer. Hence for the composite of silver and zirconium nanoparticles over graphene, good electrocatalytic activity is obtained due to the synergistic combination of nanomaterials leading to high electrical conductivity and fast electron transfer rates which is in confirmation with the above CV studies.

Electrochemical behavior of fenitrothion at Ag-ZrO$_2$-GR/GCE

Cyclic voltammetric behaviour of fenitrothion exhibited two cathodic peaks (c1 and c2) and one anodic peak (a2) in pH 2.0 using Ag-ZrO$_2$-GR/GCE over the potential range +0.4 to −1.0 V at a scan rate of 50 mVs^{-1} during the second potential scan as shown in Fig. 4a [18]. A single, irreversible reduction peak, c1, was obtained at -0.50 V due to the electrochemical reduction of nitro group to
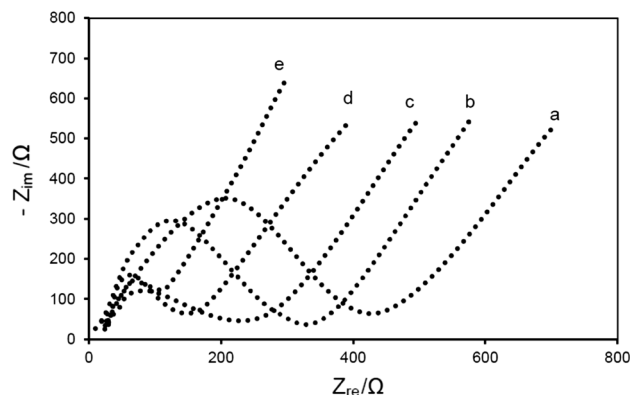

Fig. 3 Nyquist plots of ferricyanide (5 mM) in 0.1 M KCl using **a** bare GCE, **b** GR/GCE, **c** Ag-GR/GCE, **d** ZrO$_2$-GR/GCE, and **e** Ag-ZrO$_2$-GR/GCE
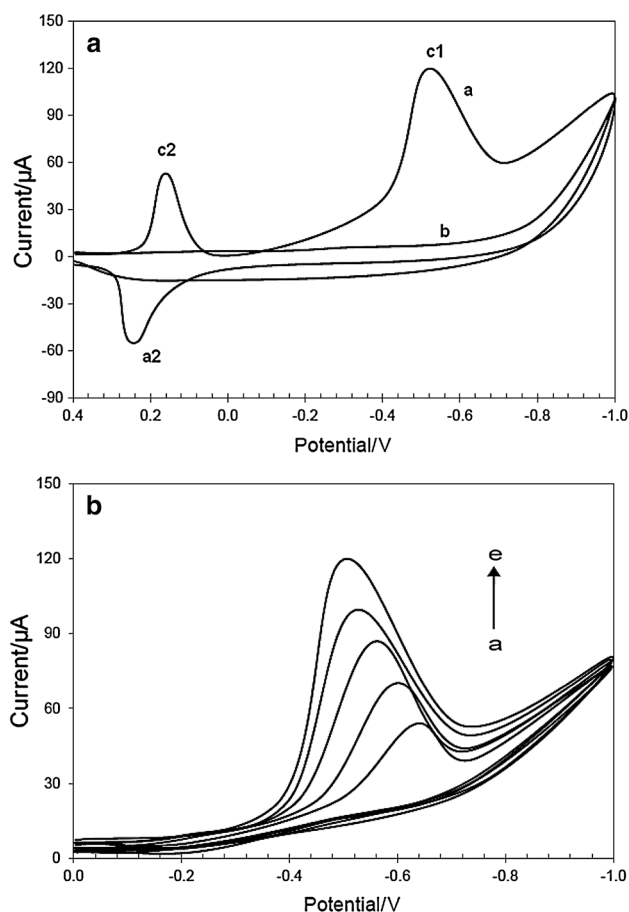

Fig. 4 a Cyclic voltammograms of second potential sweep obtained with Ag-ZrO$_2$-GR/GCE in (**a**) presence of fenitrothion (1 × 10^{-5} M) and (**b**) blank; **b** Cyclic voltammograms of fenitrothion (1 × 10^{-5} M) at bare GCE (**a**), GR/GCE (**b**), Ag-GR/GCE(**c**), ZrO$_2$-GR/GCE(**d**), Ag-ZrO$_2$-GR/GCE (**e**) in BR buffer (pH 3.0) at a scan rate of 50 mVs^{-1}

hydroxylamine. Further due to reversible conversion of hydroxylamine to nitroso group, two peaks (c2 and a2) were observed at +0.14 and +0.24 V, respectively. By

considering the maximum and well-defined cathodic peak c1, subsequent voltammetric studies were carried out. The electrocatalytic activity of the nanocomposite and other electrodes was studied as illustrated in Fig. 4b. For bare GCE, a relatively low peak current at more negative potential of -0.64 V was obtained. Improved catalytic activity was obtained for Ag-ZrO$_2$-GR/GCE (e) demonstrated by the shift of peak potential positively by 140 mV and peak current increased by 3 times in comparison to bare GCE (a). This can be explained by fast electron transfer and high electrical conductivity exhibited by Ag–ZrO$_2$—graphene nanocomposite. Further the affinity of ZrO$_2$ for phosphoric group reinforces the electrocatalytic activity of the sensor towards fenitrothion [34].

Electrochemical reduction of fenitrothion

Cyclic voltammetry experiments were further carried out to study the variation of peak currents with scan rate over the range 50–300 mVs^{-1} as shown in Fig. 5. Peak current increased linearly with scan rate and a plot of I_p vs. v led to a regression line of equation I_p (μA) $= 0.126\ v$ (mVs^{-1}) $+ 68.46$ with correlation coefficient $R^2 = 0.992$. This suggests that the electrochemical reduction is adsorption-controlled.

According to the Laviron theory for a totally irreversible system [39], the cathodic peak potential, E_{pc} is related to ln v by the following expression:

$$E_{pc} = E^o + RT/\alpha nF\ \ln RTk_s/\alpha nF - RT/\alpha nF\ln v \qquad (2)$$

where α is the electron transfer coefficient, n is the number of electrons transferred, k_s is the rate constant in s^{-1}, E^o is the formal potential while R, T, and F have their usual meanings.

The increase in potential scan rate resulted in a peak potential shift to more negative values and a plot of E_p vs. ln v gave a regression line of equation
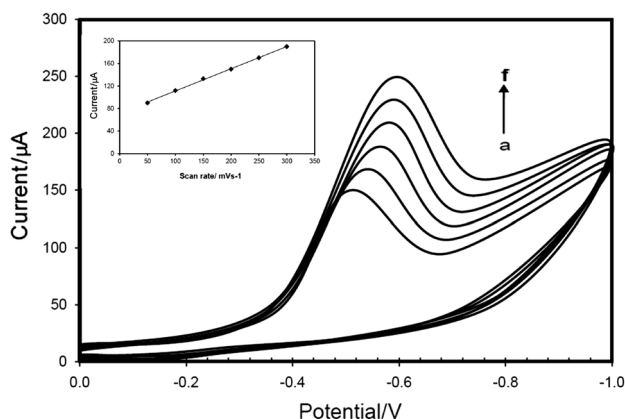

Fig. 5 Cyclic voltammetric curves for fenitrothion (1×10^{-5} M) with increasing scan rates **a** 50, **b** 100, **c** 150, **d** 200, **e** 250, **f** 300 mVs^{-1} and inset shows plot of current vs. scan rate

$$E_p = 0.011 \ln v - 0.456 \text{ with } R^2 = 0.993 \qquad (3)$$

By comparing Eqs. (1) and (2), the value of $-RT/\alpha nF = -0.011$ from which αn is calculated to be 2.317. According to Bard and Faulkner [40], for a totally irreversible reaction, electron transfer coefficient (α) is given by $\alpha = 47.7/(E_{Pc} - E_{Pc/2})$ mV^{-1} where $E_{pc/2}$ is the potential at which the peak current is half its initial value, from which the value of α is calculated to be 0.58. Since $\alpha n = 2.317$, the number of electrons, n involved in the reduction of fenitrothion to corresponding hydroxylamine is calculated to be 4.

Volume of applied casting solution and its composition

The peak signals of fenitrothion (100 nM) depend on the volume of applied casting solution and the amount of silver and zirconia nanoparticles along with graphene used in the fabrication of nanocomposite. The volume of casting solution was tested over the range 1–10 mm^3 by square wave voltammetry. An optimum volume of 5 mm^3 was used for the fabrication where high peak current was obtained (Fig. 6a). Volumes >5 mm^3 give film that might block electron transfer between the electrode and fenitrothion. Further, the amount of silver and zirconia nanoparticles were tested over the range 0.5–3.0 mg and the optimum amounts were found to be 1 and 2 mg, respectively, giving maximum peak current (Fig. 6b). Again by keeping the amount of silver and zirconia nanoparticles constant, the concentration of graphene was varied over range 0.5–3.0 mg/cm^3 in nafion (0.6 W %) solution. Maximum peak currents were obtained with concentration of 1 mg/cm^3 (Fig. 6c).

The effect of nafion on peak currents was also studied for fenitrothion over the range 0.2–1.0 W % using square wave voltammetry. Peak current increased from 0.2 to 0.6 W % and beyond that it decreased (Fig. 6d). Due to the presence of nafion, attraction of negatively charged sulfonated groups for protonated fenitrothion molecules increases the interactions with electrode surface. At amounts >0.6 W %, an insulating thick film of nafion was formed that might increase the resistance to mass and charge transfer leading to low peak currents [20].

Role of pH

The availability of protons in the test solution is crucial for the electrochemical reduction of nitro group (–NO$_2$) containing fenitrothion. The reduction peak current of fenitrothion was tested using square wave voltammetry over BR buffer of pH range 2–10 as shown in Fig. 7. Increase in peak current was observed when the pH was changed from 2.0 to 3.0 and then decreased from pH 3.0 to
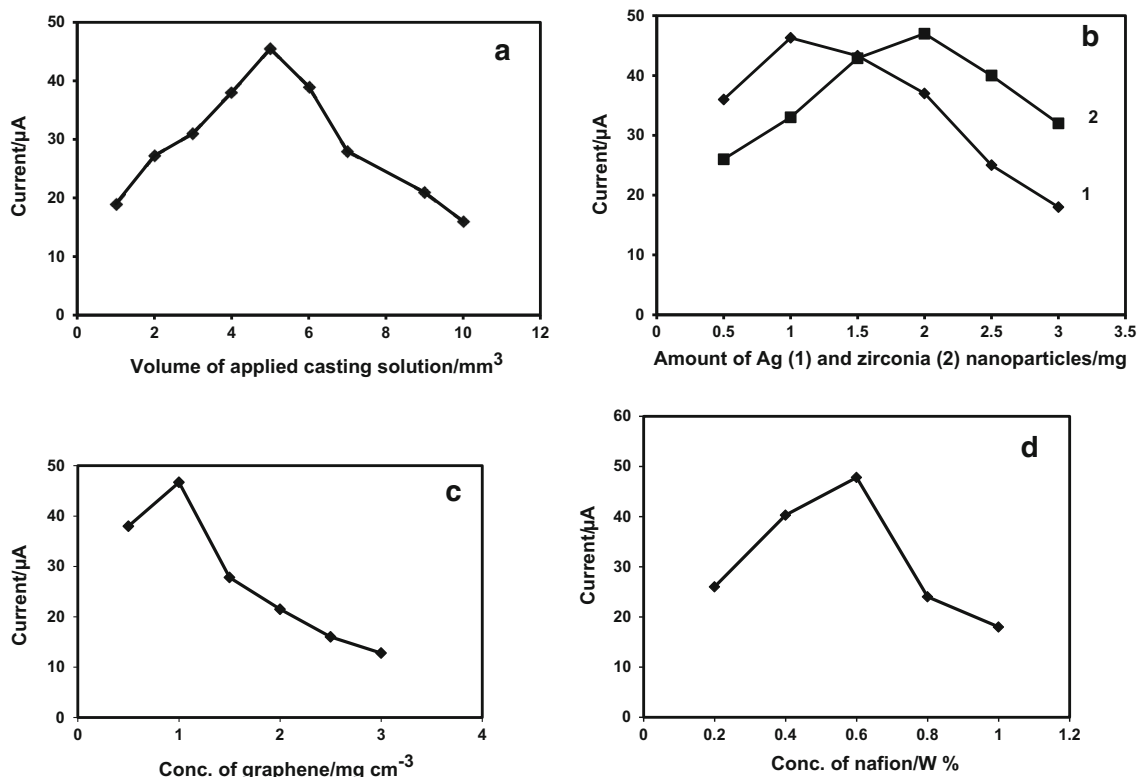
Fig. 6 Effect of volume of applied casting solution in mm^3 (**a**), amount of Ag (*1*) and ZrO$_2$ (*2*) in mg (**b**), conc. of graphene in mg/cm^3 (**c**) and conc. of nafion in W % (**d**) on peak current of fenitrothion

10.0. Hence an optimum pH of 3.0 was selected for subsequent studies where the compound showed more reproducible peak signal. Further negative shift in peak potential was observed with increase in pH demonstrating proton participation. The slope of peak potential vs. pH plot gave a value of 59 mV/pH indicating proton–electron equivalence, which is 4e- and 4H$^+$ in the case of irreversible reduction of nitro group to hydroxyl amine.
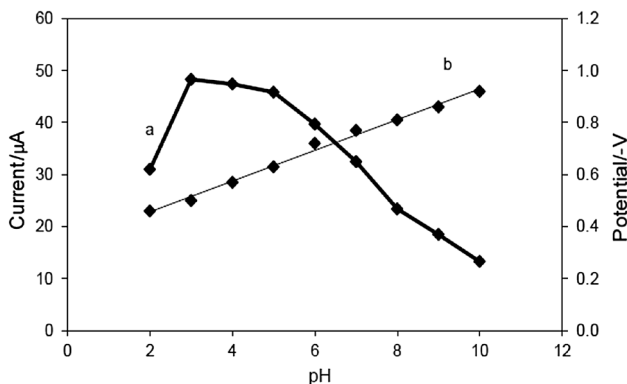

Fig. 7 Effect of pH on peak current (**a**) and peak potential (**b**) of fenitrothion (100 nM) using Ag-ZrO$_2$-GR/GCE

Pre-concentration step conditions

In the pre-concentration step, the accumulation potential (E_{acc}) of working electrode was varied from -0.05 to -0.3 V in the presence of fenitrothion (100 nM) at a constant accumulation time of 90 s. The peak current increased resulting in maximum value at -0.2 V and then decreased as shown in Fig. 8a. Hence accumulation potential of -0.2 V was selected for further SWV studies.

Again square wave voltammetric measurements were used to study the effect of accumulation time (t_{acc}) over the range of 0–180 s at constant accumulation potential of -0.2 V. As shown in Fig. 8b, the peak current increased with accumulation time from 0 to 90 s for the pre-concentration of fenitrothion over the surface of Ag-ZrO$_2$-GR/GC electrode. Maximum peak current was obtained at 90 s and with further increase in accumulation time, the peak current leveled off. This indicates that adsorption equilibrium is reached for fenitrothion over the nanocomposite. Further rapid deposition of analyte at short time can be explained due to the affinity of phosphoric group containing fenitrothion for zirconia nanoparticles of nanocomposite.
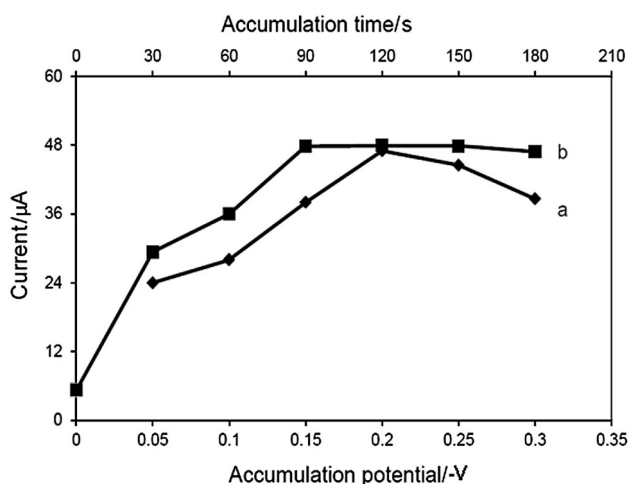
Fig. 8 Effect of **a** accumulation potential at constant accumulation time of 90 s and **b** accumulation time at constant accumulation potential of −0.2 V on the peak current of fenitrothion (100 nM)
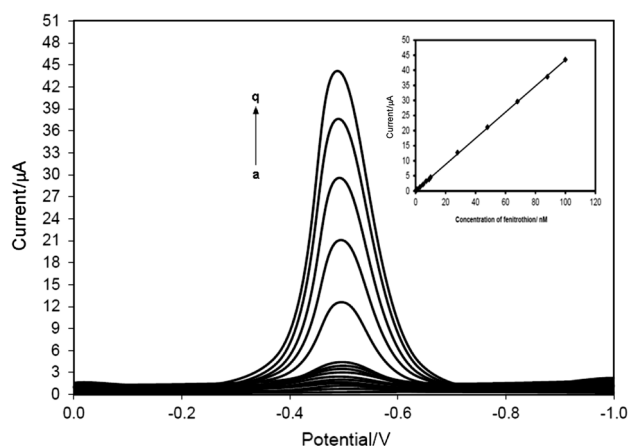

Fig. 9 Square wave adsorptive stripping voltammograms of fenitrothion at concentrations **a** 0.0, **b** 0.1, **c** 0.3, **d** 0.5, **e** 0.7, **f** 0.9, **g** 1.0, **h** 3.0, **i** 5.0, **j** 7.0, **k** 9.0, **l** 10, **m** 28, **n** 48, **o** 68, **p** 88, **q** 100 nM and inset shows calibration plot of current vs. concentration of fenitrothion

Square wave pulse parameters

The effect of square wave amplitude on peak current was studied from 10 to 100 mV. Maximum peak current was obtained at 50 mV and was selected for the determination of fenitrothion. A square wave frequency of 40 Hz was selected over a range of 10–100 Hz based on maximum peak currents and peak shapes. At frequencies higher than 40 Hz, peak distortion occurred although peak current increased (data not shown). Further the optimum values of step potential, rest period and stirring rate were 5 mV, 10 s, and 300 rpm, respectively, based on maximum peak currents and good peak shapes.

Calibration range

The variation of peak current with the concentration of fenitrothion over the range 0.1 to 100 nM was studied in BR buffer (pH 3.0). The peak signals were recorded by square wave adsorptive stripping voltammetry using Ag-ZrO_2-GR/GCE under the above optimum conditions as shown in Fig. 9. A plot of peak current against concentration of fenitrothion over the tested range was found to be linear with regression equation, I_p (µA) $= 0.432$ C (nM) $+ 0.151$, $R^2 = 0.999$. The detection limits were found to be 0.56 nM based on $3S_a/m$, where S_a is the standard deviation of y-intercept and 'm' is the slope of the calibration line.

Stability, reproducibility, and selectivity of the electrode

The electrode was stored in air at room temperature for 30 days after which the change in peak signal of fenitrothion was found to be less than 10 %. The reproducibility of the electrode fabrication was determined by measuring the response of ten different electrodes made by identical fabrication method. This led to RSD value of 3.8 % indicating good reproducibility of electrode fabrication. RSD values for inter-day assay and intra-day assay (repeatability) values of the electrode were 4.7 and 3.5 %, respectively, which were obtained by carrying out single determination of fenitrothion on 10 consecutive days and 10 measurements on a single day. Hence the developed electrode demonstrated high stability and reproducibility. In order to check the selectivity, the effect of 50-fold concentration (5000 nM) of *o*-, *m*-, *p*-nitrophenols, nitrobenzene, and *o*-, *m*-, *p*-nitroaniline on peak signal of fenitrothion (100 nM) was investigated. The peak signals for *o*-, *m*-, *p*-nitrophenols were obtained at -0.62, -0.64, and -0.69 V. Again for nitrobenzene, *o*-, *m*-, *p*-nitroaniline, the peak signals were at −0.71, −0.66, −0.68, and −0.73 V, respectively. However, the peak signals of the above compounds showed little effect (relative percentage error <5 %) on the peak current of fenitrothion. This might be due to the affinity of the nanocomposite electrode to phosphoric moiety of fenitrothion compared to other nitro compounds tested. Hence the electrode exhibited sufficient selectivity among compounds having similar electroactive functional group.

Interferences and comparison studies

The effect of inorganic ions and locally used pesticides over the peak signals of fenitrothion was studied. It was found that the peak signal was unaffected in the presence of

Table 1 Comparison of analytical performance of different modified electrodes for fenitrothion

S.No.	Electrode	Linear range/M	Detection limit/M	Method	Ref.
1	Nano-TiO$_2$ polymer/GCE[a]	2.5×10^{-8}–1×10^{-5}	1×10^{-8}	SWV[b]	[18]
2	CCE[c]	0.005–0.1	1.6×10^{-3}	SWAdSV[d]	[19]
		0.1–0.15			
3	Molecularly imprinted polymer based screen printed electrode	3×10^{-6}–1×10^{-4}	8×10^{-7}	SWV	[20]
4	Nano-TiO$_2$/Nafion/GCE	2×10^{-7}–4×10^{-6}	8.6×10^{-8}	DPV[e]	[21]
5	Polyaniline/GCE	1×10^{-8}–1×10^{-4}	7.2×10^{-9}	DPAdSV[f]	[22]
6	Electrochemically pretreated GCE	4×10^{-7}–5×10^{-5}	7.2×10^{-8}	SWAdSV	[23]
7	Poly-AHNSA[g]/GCE	1×10^{-8}–1×10^{-4}	7.95×10^{-10}	SWAdSV	[25]
8	Ag-ZrO$_2$-GR/GCE	1×10^{-10}–1×10^{-7}	5.6×10^{-10}	SWAdSV	Present work

[a] Glassy carbon electrode

[b] Square wave voltammetry

[c] Carbon ceramic electrode

[d] Square wave adsorptive stripping voltammetry

[e] Differential pulse voltammetry

[f] Differential pulse adsorptive stripping voltammetry

[g] Poly-(4-amino-3-hydroxynaphthalenesulfonic acid)

Cu^{2+}, Zn^{2+}, Pb^{2+}, Cd^{+2}, F^-, Cl^-, NO_3^-, SO_4^{2-}, and PO_4^{3-} at 500-fold concentration. Moreover, the peak signal of fenitrothion was not affected in the presence of carbamate and OP pesticides such as carbaryl, methacarb, chloropyrifos, azinphos-methyl, and fenthion at 250-fold concentration. Hence the electrode showed low interference effect by matrix components and selected pesticides during the determination of fenitrothion. As given in Table 1, based on the comparison of non-enzymatic, sensitive voltammetric sensors reported for fenitrothion, the present electrode offers wide linear range at lower concentration side with low detection limits (5.6×10^{-10} M) due to the adsorptive accumulation of fenitrothion on the Ag- ZrO$_2$-GR/GC electrode prior to the stripping step of the nanocomposite.

Application of the developed method to well water and soil samples

The method developed was directly applied for the determination of fenitrothion in well water samples and soil samples. Direct measurement of water and soil samples produced no peak signal suggesting absence of fenitrothion. Hence well water and soil samples were spiked with fenitrothion in the concentration range of 2–10 ng/cm^3 and 1–5 ng/g as explained in experimental section. The validity of the voltammetric method was investigated by recovery tests and five replicate determinations were carried out at each concentration level. As given in Tables 2 and 3, recovery ranges of fenitrothion are 92.5–98.3 % with RSD values 3.5–4.1 % for well water and 94.0–101.8 % with RSD values 2.3–3.5 % for

soil samples indicating good accuracy and precision of the developed method.

Conclusions

Ag–ZrO$_2$ based graphene nanocomposite modified glassy carbon electrode was easily fabricated and readily employed for the determination of fenitrothion. Increased peak currents and decreased peak potentials are obtained due to fast electron transfer rate, good electrical conductivity resulting from the synergistic combination of Ag and ZrO$_2$ nanoparticles over graphene backbone. The nanocomposite electrode exhibited enhanced sensitivity, selectivity, high catalytic activity, good stability, and reproducibility. The major advantages of the developed voltammetric method are that it is a simple, cheap, and rapid one offering wide linear working range and low limits of detection with fewer sample preparation steps for fenitrothion. The proposed method was successfully applied to well water and soil samples with excellent precision and accuracy as suggested by low RSD values and good recoveries. Hence the present Ag-ZrO$_2$-graphene nanocomposite could be envisaged as a potential sensor design for ultra-trace determination of fenitrothion in environmental matrices.

Experimental

Fenitrothion, silver (Ag, size: ≤100 nm, purity: 99.5 %) and zirconia (ZrO$_2$, size: ≤100 nm, purity: 99.5 %)

Table 2 Recovery tests for fenitrothion in well water sample

Sample	Added concentration/ ng cm^{-3}	Observed concentration[a]/ ng cm^{-3}	Recovery/%	RSD/%
Well water	2	1.85	92.5	3.7
	4	3.93	98.3	4.1
	6	5.87	97.8	3.9
	8	7.76	97.0	3.5
	10	9.56	95.6	3.9

[a] Average of five replicate determinations

Table 3 Recovery tests for fenitrothion in soil sample

Sample	Added concentration/ ng g^{-1}	Observed concentration[a]/ ng g^{-1}	Recovery/%	RSD/%
Soil	1	0.94	94.0	2.3
	2	1.93	96.5	2.9
	3	2.87	95.7	3.2
	4	3.89	97.3	2.6
	5	5.09	101.8	3.5

[a] Average of five replicate determinations

nanoparticles were purchased from Sigma-Aldrich, USA and graphene (GR) was obtained from DropSens, Spain. Britton-Robinson buffers (pH: 2–10) were prepared from 0.04 M solution each of orthophosphoric acid, acetic acid, boric acid and the pH was adjusted using 0.2 M NaOH solution. Other chemicals and solvents used were of analytical reagent grade and were obtained from Merck (Mumbai, India). A 1.0 mM stock solution of fenitrothion was made up in ethanol (AR-grade).

All electrochemical studies were carried out using CHI 660D workstation (CH Instruments, USA). A three-electrode system consisting of a bare glassy carbon electrode (GCE, 3 mm diameter) and a Ag-ZrO$_2$-GR nanocomposite modified GCE as working electrode, a Ag/AgCl (3 M KCl) electrode as a reference electrode and a Ag wire as counter electrode were used. An Elico LI-120 pH meter with a combined glass electrode was used to measure the pH of the buffer and test solutions. All measurement steps were carried out at a temperature of 25 °C.

Preparation of Ag-ZrO$_2$-GR/GCE

The electrode substrate (glassy carbon electrode) was polished mirror-like with 0.05 μm alumina slurry, rinsed with triple distilled water to remove alumina particles, and dried under nitrogen. It was subsequently rinsed with ethanol and triple-distilled water followed by drying. Ag nanoparticles (1 mg) and ZrO$_2$ nanoparticles (2 mg) were

added to graphene (1 mg) in 1 cm^3 of Nafion (0.6 wt %) solution. The mixture was sonicated for 25 min until a black, homogeneous suspension was obtained. The resultant dispersion (5 mm^3) was drop-casted on GCE followed by drying under nitrogen gas at room temperature. The nanocomposite sensor was rinsed with triple-distilled water to remove loosely adhering layers and dried. It was first characterized with cyclic voltammetry and impedance technique using [Fe(CN)$_6$]$^{3-}$ system in presence of KCl. Finally, it was taken for the determination of fenitrothion by square wave adsorptive stripping voltammetry. Similarly, different modified electrodes such as GR/GCE, Ag-GR/GCE, and ZrO$_2$-GR/GCE were prepared as described by the above drop-cast method for comparing their electrochemical performance with the present nanocomposite sensor.

Voltammetric procedure for fenitrothion determination

A working standard of fenitrothion (100 nM) was prepared from the stock solution using double distilled water. A blank BR buffer (pH 3.0) purged with nitrogen gas for 15 min was measured with the Ag-ZrO$_2$-GR/GC electrode before any measurement of fenitrothion. Test solution containing 1.0 cm^3 of the working standard and 9.0 cm^3 of the BR buffer (pH 3.0) was taken into the electrolytic cell and purged with nitrogen gas. The electrode was kept at −0.2 V for a period of 90 s during pre-concentration step. In the stripping step, the potential of Ag-ZrO$_2$-GR/GC electrode was scanned from 0.0 to −1.0 V using square wave voltammetry (SWV). After each measurement, the sensor is regenerated by multiple SWV stripping scans in blank BR buffer (pH 3.0) until no peak appeared and then washed twice with double distilled water, and dried. The optimum working and instrumental conditions were as follows: pH: 3.0, E_{acc}: −0.2 V, t_{acc}: 90 s, square wave frequency: 40 Hz, square wave amplitude: 50 mV, step potential: 5 mV, scan range: 0.0 to −1.0 V, and concentration range of fenitrothion: 0.1 to 100 nM.

Preparation of well water and soil samples

A spiking stock solution (100 mg/cm^3) of fenitrothion was prepared in ethanol from which working standards of concentrations, 10 and 1 μg/cm^3 were prepared using double-distilled water. Well waters (50 cm^3) collected were filtered through 0.45 μm paper and stored at 4 °C. Water samples (5 cm^3) were spiked with standard pesticide solution to get concentration range of 2–10 ng/cm^3. It was directly added to 5 cm^3 of BR buffer (pH 3.0) and subjected to voltammetric procedure.

Soil samples (50 g) collected were washed twice with double-distilled water, air-dried and pulverized in a mortar.

A portion of soil samples (5 g) was spiked with working standard solution to get fenitrothion concentration of 1–5 ng/g. Spiked soil sample was mixed well and extracted with 25 cm^3 of acetone under mechanical shaking for 30 min. The extract was filtered and evaporated on water bath. The residue is redissolved in 2 cm^3 of ethanol. Finally, it was added to electrolytic cell containing 8 cm^3 of BR buffer (pH 3.0) for voltammetric measurement.

References

1. Benli ACK, Özkul A (2010) Pestic Biochem Physiol 97:32
2. Sarikaya R, Dinçel AS, Benli ACK, Selvi M, Erkoç F (2011) J Biochem Mol Toxicol 25:169
3. Story P, Hooper MJ, Astheimer LB, Buttemer WA (2011) Environ Toxicol Chem 30:1163
4. Ahmadi F, Jafari B (2011) Electroanalysis 23:675
5. Sánchez A, Millán S, Sampedro MC, Unceta N, Rodríguez E, Goicolea MA, Barrio RJ (2008) J Chromatogr A 1177:170
6. Pitarch E, Serrano R, López FJ, Hernández F (2003) Anal Bioanal Chem 376:189
7. Morzycka Bozena (2002) J Chromatogr A 982:267
8. Ahmadi F, Assadi Y, Milani Hosseini SMR, Rezaee M (2006) J Chromatogr A 1101:307
9. Ortega AS, Sampedro MC, Unceta N, Goicolea MA, Barrio RJ (2005) J Chromatogr A 1094:70
10. Galeano-Díaz T, Guiberteau-Cabanillas A, Mora-Díez N, Parrilla-Vázquez P, Salinas-López F (2000) J Agric Food Chem 48:4508
11. Pereira LA, Rath S (2009) Anal Bioanal Chem 393:1063
12. Chunxia Wu, Liu Ning, Qiuhua Wu, Wang Chun, Wang Zhi (2010) Anal Chim Acta 679:56
13. Kim YJ, Kim YA, Lee YT, Lee HS (2007) Anal Chim Acta 591:183
14. Coly A, Aaron JJ (1994) Analyst 119:1205
15. Pawlak MK (2004) Polish J Environ Studies 13:411
16. Melgar LZ, Machado SAS (2005) J Braz Chem Soc 16:743
17. Galeano-Díaz T, Guiberteau-Cabanillas A, Espinosa-Mansilla A, López-Soto MD (2008) Anal Chim Acta 618:131
18. Li C, Wang C, Ma Y, Hu S (2004) Microchim Acta 148:27
19. Majidi MR, Asadpour-Zeynali K, Nazarpur M (2009) J AOAC Int 92:548
20. Pellicer C, Gomez-Caballero A, Unceta N, Goicolea AM, Barrio RJ (2010) Anal Methods 2:280
21. Kumaravel A, Chandrasekaran M (2011) J Electroanal Chem 650:163
22. Sreedhar NY, Reddy Prasad P, Nageswara Reddy C, Sreenivasa Prasad K (2011) Int J Nanosci Nanotechnol 1:6
23. Geremedhin W, Amare M, Admassie S (2013) Electrochim Acta 87:749
24. Palazzo F, Codognoto L, Simões FR (2013) Sens Lett 11:2310
25. Amare M, Abicho S, Admassie S (2014) J AOAC Int 97:580
26. Shao Y, Wang J, Wu H, Liu J, Aksay IA, Lin Y (2010) Electroanalysis 22:1027
27. Ma H, Wu D, Cui Z, Li Y, Zhang Y, Du B, Wei Q (2013) Anal Lett 46:1
28. Katz E, Willner I, Wang J (2004) Electroanalysis 16:19
29. Luo X, Morrin A, Killard AJ, Smyth MR (2006) Electroanalysis 18:319
30. Wang F, Hu S (2009) Microchim Acta 165:1
31. Wang J (2012) Microchim Acta 177:245
32. Merkoçi A (2013) Electroanalysis 25:15
33. Lu X, Qi H, Zhang X, Xue Z, Jin J, Zhou X, Liu X (2011) Chem Commun 47:12494
34. Liu G, Lin Y (2005) Anal Chem 77:5894
35. Gong J, Miao X, Zhou Z, Zhang L (2011) Talanta 85:1344
36. Du D, Liu J, Zhang X, Cui X, Lin Y (2011) J Mater Chem 21:8032
37. Wang K, Li HN, Wu J, Ju C, Yan JJ, Liu Q, Qiu B (2011) Analyst 136:3349
38. Yang L, Wang G, Liu Y (2013) Anal Biochem 437:144
39. Laviron E (1979) J Electroanal Chem 101:19
40. Bard AJ, Faulkner LR (2004) Electrochemical methods: fundamentals and applications, 2nd edn. Wiley, New York